Glauber model for transfer reactions

F. Carstoiu,* C. Lazard, and R. J. Lombard
Division de Physique Théorique, Institut de Physique Nucléaire, 91406 Orsay Cedex, France
(Received 7 January 1998)

We investigate two aspects of the Glauber model for (p,d) transfer reactions on nuclei. The first one is connected with the violation of angular momentum conservation at the transition vertex inherent to straight line propagation. This can be cured by introducing a different impact parameter in the entrance and exit channels. We give an estimate of this effect in the case of (p,d) reactions on ^{12}C. Second, the formalism is applied to single neutron halo nuclei. We study the sensitivity of the (p,d) cross sections to the radial dependence of the halo wave function and to its rms radius. [S0556-2813(98)05306-0]

PACS number(s): 25.40.Hs, 24.10.Eq, 21.10.Pc, 27.20.+n

I. INTRODUCTION

Transfer reactions have been widely used to investigate nuclear structure. At low energy, the data analysis is usually performed by means of distorted-wave Born approximation (DWBA) techniques or coupled channel calculations. At intermediate energies, the hope of learning more about nuclear structure once the reaction mechanism is under control has been emphasized by Wilkin [1]. He showed the triangular graph model to be quite successful in connecting different transfer reactions.

To our knowledge, little effort has been made to formulate the approach in the impact parameter representation. Of particular interest in this domain is the paper by Shepard and Rost [2] dealing with (p,d) and (d,p) reactions at 800 MeV. Starting from the eikonalization of the zero-range DWBA amplitude, they developed an analytical expression similar to that of Amado, Dedonder, and Lenz [3] devoted to elastic scattering. Their approach allows us to understand the salient and systematic features of transfer reactions at intermediate energies. Recently, a simplified eikonalized DWBA transfer amplitude has been used by Bayman *et al.* [4] to study finite range effects, a point of importance in the case of heavy ion transfer reactions.

The purpose of the present work is to provide a formulation of the (p,d) reaction in the Glauber model. The extension from the usual elastic scattering prescription to processes involving a nuclear transition is straightforward. The major difficulty is the fact remarked a while ago by Formanek [5] that the Glauber model does not preserve time reversal and unitarity as soon as longitudinal momentum transfers (mass transfer) occur in the reaction. This traces back to imposing straight line propagation, which violates classical angular momentum conservation at the transition vertex. As long as the stripping and pickup reactions are dominated by a two-channel process, this can be remedied in a simple way, by allowing a different value of the impact parameter in the entrance and exit channels [6,7] proportional to

$$\lambda = k_f / k_i ,$$

namely, to the ratio of the outgoing and incoming particle momenta. A crude estimate has proved that indeed this effect has a noticeable influence on the shape and magnitude of the differential cross section of (p,d) reactions at intermediate energies [8].

Our first aim is to revisit this question and to give a better estimate of the influence of λ. We shall also compare this effect to corrections arising from noneikonal propagation in the entrance and exit channels.

Furthermore, because of the current interest in halo nuclei, we will consider the case of the (p,d) reaction on a target made of a neutron very weakly bound to a core. Halo nuclei are very unstable and are known to be characterized by large dissociation cross sections, which increase with the square radius of the halo wave function [9]. On this naive ground, we expect also a large amount of transfer reactions. Thus it is interesting to check their potentialities.

The paper is organized as follows. In Sec. II, the basic formulas are given. Section III is devoted to (p,d) reactions on ^{12}C as a test of the importance of the corrections advocated in this Introduction. In Sec. IV, we discuss the (p,d) reaction on ^{11}Be taken as the archetype of single neutron halo nuclei. Conclusions are drawn in Sec. V.

II. MODEL

In the Glauber model, the differential cross section for the $A(p,d)B$ reaction is given by

$$\frac{d\sigma}{d\Omega} = \frac{1}{(2\pi\hbar^2)^2} \frac{w_p w_A}{w_p + w_A} \frac{w_d w_B}{w_d + w_B} \frac{k_d}{k_p} S \sum_m |T_{lm}(\vec{q}, q_\parallel)|^2, \tag{1}$$

where S contains spin and possibly spectroscopic factors. The neutron is assumed to be picked from a quantum state of angular momentum l and projection m with respect to the core (residual) nucleus. The quantity $w_j = \sqrt{m_j^2 + \hbar^2 k_j^2}$ is the total energy of the particle $j(p,\ A,\ d,$ or $B)$; k_p and k_d are the momentum of the proton and deuteron, respectively. The z axis is directed along the incident momentum $\vec{k}_p$. The total momentum transfer $\vec{Q} = \vec{k}_p - \vec{k}_d$ has transverse and longitudi-

*Permanent address: Department of Fundamental Physics, Institute for Physics and Nuclear Engineering, Magurele-Bucharest, MG-6, R-76900, Romania.

nal components $\vec{q}$ and $q_\parallel$, respectively. Note that we shall adopt the small angle approximation. In this case, the longitudinal component is kept to its minimal value

$$q_\parallel = k_p - k_d,$$

and the scattering angle is related to the norm of the perpendicular momentum transfer,

$$q = k_d \sin\vartheta.$$

We neglect also nucleon binding energies, which could be of importance in actual cases, while calculating kinematical quantities. The transition matrix element is given by

$$T_{lm}(\vec{q},q_\parallel) = \int e^{i\vec{q}\cdot\vec{b}} \Gamma^{dp}(\vec{b},q_\parallel) d^2b, \tag{2}$$

where $\Gamma^{dp}(\vec{b},q_\parallel)$ is the total profile function. It is obtained from averaging over the nuclear coordinates of the time ordered product of the elementary profile functions. In a two-channel approach, the S matrix describing the interaction of the propagating particle with each target nucleon at position $\vec{x}=(\vec{s},z)$ is written as a 2×2 matrix in the impact parameter representation

$$S(\vec{b},\vec{x}) = \begin{pmatrix} S^{pp}(\vec{b}-\vec{s}) & \lambda S^{pd}(\vec{b}-\vec{s}) e^{-iq_\parallel z} \\ \frac{1}{\lambda} S^{dp}\left(\frac{\vec{b}}{\lambda}-\vec{s}\right) e^{iq_\parallel z} & S^{dd}\left(\frac{\vec{b}}{\lambda}-\vec{s}\right) \end{pmatrix}. \tag{3}$$

The factor $\lambda = k_d/k_p$ takes care of the conservation of the classical angular momentum at the transition vertex,

$$\vec{k}_p \times \vec{b}' = \vec{k}_d \times \vec{b}.$$

As explained in [6], use is made here of the ambiguity in the definition of the impact parameter, which can be defined either in the entrance or in the exit channel, to satisfy the classical conservation law.

We recall that the submatrices $S^{kj}(\vec{b})$ are related to the corresponding profile functions by

$$S^{kj}(\vec{b}) = \delta_{kj} - \gamma^{kj}(\vec{b}). \tag{4}$$

In the set of indices $\{k,j\}$, the latter represent the initial state of the propagating particle, the former the final state. Consequently, in Eq. (3), S^{pp} and S^{dd} correspond to proton and deuteron elastic scattering, while S^{pd} and S^{dp} describe the (d,p) and (p,d) interaction vertices, respectively.

The time-ordered product of the individual S matrix must be taken with care, since in general the S matrix elements do not commute. The appropriate expression of the total S matrix for fixed nucleon positions is given by

$$S(\vec{b},\vec{x}_1,\ldots,\vec{x}_A) = \sum_{perm} \theta(z_{i_A}-z_{i_{A-1}}) \cdots \theta(z_{i_3}-z_{i_2}) \times \theta(z_{i_2}-z_{i_1}) S(\vec{b},\vec{x}_{i_A}) \cdots S(\vec{b},\vec{x}_{i_1}), \tag{5}$$

where the sum runs over all permutations $\{i_1,\ldots,i_A\}$ of $1,\ldots,A$.

A few well-justified assumptions greatly reduce the complexity of the total profile function. Because of the large momentum transfer at each transition vertex, we retain only terms linear in γ^{dp}. We neglect the spin dependence of the profiles functions. In such a case all terms commute and we end up with

$$\Gamma^{dp}(\vec{b},q_\parallel) = \langle \Psi_B(\vec{x}_1,\ldots,\vec{x}_{i-1},\vec{x}_{i+1},\ldots\vec{x}_A) | \times \hat{\Gamma}(\vec{b},\vec{x}_1\cdots\vec{x}_A) | \Psi_A(\vec{x}_1,\ldots,\vec{x}_A)\rangle, \tag{6}$$

where

$$\hat{\Gamma}(\vec{b},\vec{x}_1\cdots\vec{x}_A) = \sum_i \gamma^{dp}(\vec{b}-\vec{s}_i) e^{iq_\parallel z_i} \times \prod_{k\neq i} [1-\gamma^{dd}(\vec{b}-\vec{s}_k)\theta(z_k-z_i) - \gamma^{pp}(\lambda\vec{b}-\vec{s}_k)\theta(z_i-z_k)]. \tag{7}$$

Neglecting center-of-mass corrections, and assuming a naive shell model picture of the nucleus, we write

$$\Psi_A(\vec{x}_1,\ldots,\vec{x}_A) = \Psi_B(\vec{x}_1,\ldots,\vec{x}_{i-1},\vec{x}_{i+1},\ldots,\vec{x}_A) \times \Phi_{\not m}(\vec{x}_i).$$

Here $\Phi_{lm}(\vec{x}_i)$ is the wave function of the captured particle. We consider the reaction to take place on a single nucleon. More precisely, the pickup process is supposed to be specific to a single shell. Consequently we shall drop the sum over the index i in Eq. (7), the possible multiplicity of equivalent nucleons being taken into account in the factor S of Eq. (1). Under these assumptions, the total profile function becomes

$$\Gamma^{dp}(\vec{b},q_\parallel) = \int d^2s_i dz_i \gamma^{dp}(\vec{b}-\vec{s}_i) e^{iq_\parallel z_i} \Phi_{\not m}(\vec{s}_i,z_i) \prod_{k\neq i} \times \int d^2s_k dz_k \rho(\vec{s}_k,z_k) [1-\gamma^{dd}(\vec{b}-\vec{s}_k)\theta(z_k-z_i) - \gamma^{pp}(\lambda\vec{b}-\vec{s}_k)\theta(z_i-z_k)], \tag{8}$$

where $\rho(\vec{x})$ is the single particle density. Instead of dealing with a microscopic calculation of the elastic part, it is very appropriate to introduce the optical limit

$$\Gamma^{dp}(\vec{b},q_\parallel)$$

$$= \int d^2s\,dz\,\gamma^{dp}(\vec{b}-\vec{s})e^{iq_\parallel z}\Phi_{\ell m}(\vec{s},z)$$

$$\times\exp\left(-A\int d^2s'dz'\rho(\vec{s}',z')\gamma^{dd}(\vec{b}-\vec{s}')\theta(z'-z)\right)$$

$$\times\exp\left(-A\int d^2s'dz'\rho(\vec{s}',z')\gamma^{pp}(\lambda\vec{b}-\vec{s}')\theta(z-z')\right). \tag{9}$$

The exponentiation allows us to introduce in a natural way the optical phase in the entrance and exit channels by setting

$$A\int d^2s'\rho(\vec{s}',z')\gamma^{dd}(\vec{b}-\vec{s}') = -i\chi_d(\vec{b},z'), \tag{10}$$

$$A\int d^2s'\rho(\vec{s}',z')\gamma^{pp}(\lambda\vec{b}-\vec{s}') = -i\chi_p(\vec{b},z'). \tag{11}$$

At the lowest order, the total phase $\chi(\vec{b},z)=\chi_p(\vec{b},z)+\chi_d(\vec{b},z)$ can be taken as the eikonal approximation

$$\chi(\vec{b},z)\simeq\chi_0(\vec{b},z) = -\frac{m_p}{\hbar^2k_p}\int_{-\infty}^{z}V_p(\lambda\vec{b},z')dz'$$

$$-\frac{m_d}{\hbar^2k_d}\int_{z}^{\infty}V_d(\vec{b},z')dz'. \tag{12}$$

Corrections for noneikonal propagation can be included in a systematic way following Wallace [10] or Waxman *et al.* [11].

By identifying V_p and V_d with the measured optical potential of proton-nucleus A and deuteron-nucleus B elastic scattering, this procedure has the advantage of summing up a number of diagrams not explicitly written in Eq. (8). In particular the contributions involving pion degrees of freedom in the intermediate steps of the multiple scattering are automatically included. According to Eq. (8), the nucleon undergoing the transition is singled out, and, in the entrance channel, the optical potential should correspond to elastic scattering of the incoming proton colliding with the $(A-1)$ remaining nucleons. Whereas such a subtlety is irrelevant to the point we shall raise in the next section devoted to (p,d) on ^{12}C, it does matter in the case of halo nuclei and will be taken into account.

At intermediate and high energies, it is customary to simulate a relativistic wave equation by replacing in the Schrödinger equation the mass by the energy $w=\sqrt{m^2+\hbar^2k^2}$, as recommended by Newton a while ago [12]. We shall adopt this procedure in this work, with the consequence of changing m by w in the calculation of the eikonal phase.

In order to keep the numerical effort at a reasonable level, we approximate the transition profile function by a zero-range interaction

$$\gamma^{dp}(\vec{b}-\vec{s}) = D_0\delta^{(2)}(\vec{b}-\vec{s}), \tag{13}$$

which is justified in view of the aims of the present works. Analysis of actual data may require a finite range profile function. It will increase the dimensionality of the integration to be performed numerically but it is not expected to modify qualitatively our conclusions. Thus the final expression we are studying is given by

$$T_{lm}(\vec{q},q_\parallel) = D_0\int d^2b e^{i\vec{q}\cdot\vec{b}}\int_{-\infty}^{\infty}dz e^{iq_\parallel z}e^{i\chi(\vec{b},z)}\Phi_{\ell m}(\vec{b},z). \tag{14}$$

Apart from the correction factor λ, Eqs. (12) and (14) are similar to the eikonalized DWBA expression used by Shepard and Rost [2]. Note, however, that our kinematics differ slightly from the one used by these authors.

We shall end up this section with the following remark. At the level of the elementary transition profile function, T invariance requires that [6]

$$\gamma^{pd}(\vec{b}) = \frac{1}{\lambda^2}\gamma^{dp}\left(\frac{\vec{b}}{\lambda}\right). \tag{15}$$

The profile function analogous to Eq. (9) for the (d,p) reaction is given by

$$\Gamma^{pd}(\vec{b},q_\parallel)$$

$$= \frac{1}{\lambda^2}\int d^2s\,dz\,\gamma^{dp}\left(\frac{\vec{b}}{\lambda}-\vec{s}\right)e^{iq_\parallel z}\Phi^*_{lm}(\vec{s},-z)$$

$$\times\exp\left[-A\int d^2s'dz'\rho(\vec{s}',-z')\gamma^{dd}\left(\frac{\vec{b}}{\lambda}-\vec{s}'\right)\theta(z'-z)\right]$$

$$\times\exp\left(-A\int d^2s'dz'\rho(\vec{s}',-z')\gamma^{pp}(\vec{b}-\vec{s}')\theta(z-z')\right), \tag{16}$$

where z as been changed to $-z$ as well as z' to $-z'$.

In the zero-range limit (13) under the constraint (15), the (d,p) transition profile function becomes

$$\gamma^{pd}(\vec{b}-\vec{s}) = \frac{1}{\lambda^2}D_0\delta^{(2)}\left(\frac{\vec{b}}{\lambda}-\vec{s}\right). \tag{17}$$

Assuming spherical symmetry, the nuclear densities depending only on the magnitude of $\vec{x}$, we have $\rho(\vec{s'},-z')=\rho(\vec{s'},z')$, and furthermore $\Phi^*_{lm}(\vec{s},-z)=\Phi_{lm}(\vec{s},z)$. It is then easy to check that the total profile functions satisfy the time reversal invariance condition

$$\Gamma^{pd}(\vec{b},q_\parallel) = \frac{1}{\lambda^2}\Gamma^{dp}\left(\frac{\vec{b}}{\lambda},q_\parallel\right). \tag{18}$$

The validity of this relationship is not restricted to the use of zero-range transition profile functions but is quite general, as can be verified by comparing Eqs. (9) and (16).

III. ^{12}C$(p,d)^{11}$C EXAMPLE

As a practical example to test the influence of the factor λ on the transition matrix element (14), we consider (p,d) reactions on ^{12}C at an incident energy of 800 MeV. The neutron will be picked up from a $1s$ or $1p$ shell model state of ^{12}C ($l=0,1$), the radial dependence of the wave function being taken from the harmonic oscillator

$$\Phi_{lm}(\vec{r}) = 2\frac{\alpha^{3/2}}{\pi^{1/4}}\left[\sqrt{\frac{2}{3}}\alpha r\right]^l e^{-\alpha^2 r^2/2} Y_{lm}(\vartheta,\varphi)$$

$$= \phi_l(r)\Theta_{lm}(\vartheta)\frac{1}{\sqrt{2\pi}}e^{im\varphi} \tag{19}$$

(we omit the principal quantum number n, since we are dealing only with $n=1$ in our applications). The parameter α is related to the size of ^{12}C, namely, $\alpha^2 = 0.3522$ fm^{-2}.

Although the p-^{12}C optical potential could be derived from experimental elastic scattering data, in the absence of d-^{11}C data we adopt for both channels the Kerman-McManus-Thaler (KMT) prescription [13], which is known to yield an excellent fit to elastic proton-nucleus elastic scattering cross sections at intermediate energies [14,15]. Assuming zero-range nucleon-nucleon interactions for simplicity, the optical potentials are given by

$$V(\vec{r}) = -\frac{\hbar^2}{2}\frac{k_{\rm lab}}{E_{\rm lab}}\sigma(i+\alpha)\rho_A(\vec{r}). \tag{20}$$

We neglect spin degrees of freedom and average over the isospin. The parameters σ and α are the strength and the Re/Im ratio of the proton-nucleon and deuteron-nucleon interactions, respectively. The target nucleus is described by its one-body density, assumed to be spherically symmetric,

$$\rho_A(r) = n_0\frac{\kappa^3}{\pi\sqrt{\pi}}e^{-\kappa^2 r^2}\left(1+\frac{4}{3}\kappa^2 r^2\right), \tag{21}$$

and normalized to the number of particles. The same expression is used for both C isotopes. Proton and neutron densities are supposed to be equal. The parameter κ is fixed by the charge rms radius, a procedure which accounts for the finite range of the nuclear forces and produces optical potentials of ranges somewhat more realistic than the point particle densities. In the case of the d-^{11}C optical potential, the parameter κ is determined in a similar way, replacing the proton charge radius by the charge radius of the deuteron.

The optical potentials take the following form:

$$V_j(r) = -V_j(0)\left(1+\frac{4}{3}\kappa_j^2 r^2\right)e^{-\kappa_j^2 r^2}(i+\alpha_j) \quad (j=p,d). \tag{22}$$

The values of parameters used in our calculations are listed in Table I.

TABLE I. Optical potential parameters for the ^{12}C$(p,d)^{11}$C reaction at 800 MeV [Eq. (23)].

	$V_p(r)$	$V_d(r)$
$V(0)$	56.125 MeV	24.15 MeV
κ	0.5935 fm^{-1}	0.4545 fm^{-1}
α	−0.2	−0.2

The phase $\chi(\vec{b},z)$ entering Eq. (14) has been calculated at the eikonal approximation by using Eq. (12) in which the masses m have been replaced by energies w, as stated above. In principle, use should be made of reduced energies, much in the same way as reduced masses are entering the Schrödinger equation of the two-body problem. However, since we ignore center-of-mass corrections in the nuclear wave functions, this effect is neglected here.

Besides the nuclear phase, the Coulomb contribution should be added. Using the potential generated by a uniform charge distribution screened at atomic distances leads to trivial integrals. As a result of the small charges involved in the reaction, the high incident energy, and the large finite transfer momentum, the Coulomb interaction has a minor effect on the amplitude and will be omitted.

Our primary aim in this section is to discuss the effect of λ. At this stage, it is also very important to compare this effect to the approximation introduced by the eikonal propagation in order to establish the hierarchy among this two corrections. To this end we have extended the calculation of $\chi(\vec{b},z)$ by including a first order correction [10,11], which in the present case reads

$$\chi_1(\vec{b},z) = -\frac{w_p^2}{\hbar^4 k_p^3}\left(1+\lambda b\frac{d}{d(\lambda b)}\right)\int_{-\infty}^{z} V_p^2(\lambda\vec{b},z')dz'$$

$$-\frac{w_d^2}{\hbar^4 k_d}\left(1+b\frac{d}{db}\right)\int_{z}^{\infty} V_d^2(\vec{b},z')dz'. \tag{23}$$

As far as the transition matrix element (14) is concerned, the integration over the angular variable φ is straightforward and we are left with

$$T_{lm}(q) = i^m\sqrt{2\pi}\int_0^\infty J_m(qb)bdb$$

$$\times\int_{-\infty}^{\infty} e^{iq_\parallel z}\phi(r)\Theta_{lm}(\vartheta)e^{i\chi(b,z)}dz, \tag{24}$$

where Θ_{lm} has to be calculated by using $\cos\vartheta = z/\sqrt{z^2+b^2}$.

The results of the present calculations are displayed in Figs. 1 and 2, where $|T_{00}(q,q_\parallel)|^2$, $|T_{10}(q,q_\parallel)|^2$, and $|T_{11}(q,q_\parallel)|^2$, respectively, are plotted against q, for $\lambda = 1.0$ and $\lambda = k_d/k_p$; here, $\lambda = 1.26$. Calculations at zero order are limited to χ_0; those at first order include also χ_1. They confirm the earlier findings of Ref. [8]. In brief, the effect of λ is to change both the diffractive character and the magnitude of

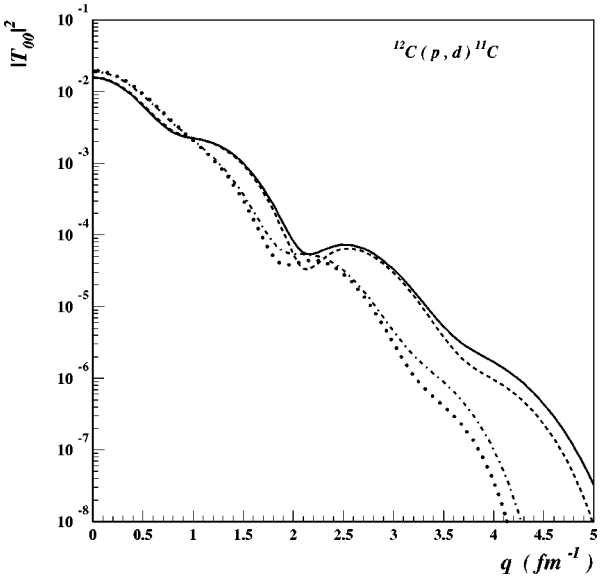

FIG. 1. (p,d) reaction on ^{12}C at 800 MeV incident energy. $|T_{00}|^2$ in arbitrary units is plotted against the magnitude of the transverse momentum transfer q. For $\lambda=1$, the dotted line corresponds to the eikonal approximation and the dot-dashed line includes the first order correction to the eikonal approximation. For $\lambda=k_d/k_p$, the dashed line corresponds to the eikonal approximation and the solid line includes the first order correction.

the differential cross section. The increase is spectacular at large angles, reaching at certain places several orders of magnitude. This behavior is well illustrated by Fig. 3, which displays the ratios $|T_{lm}(\lambda=k_d/k_p)|^2/|T_{lm}(\lambda=1)|^2$. For the $1s$ state, the effect is already manifest at $q=0$, whereas for p states it becomes noticeable only beyond 0.7 fm^{-1}.

Another striking feature is the fact that the influence of χ_1 is small, independent of λ, and does not manifest strongly in the diffraction pattern. Thus both effects are additive, and the eikonal approximation is certainly sufficient over the range of momentum transfer considered in this work.

It is very tempting to try a systematic expansion around $\lambda=1$. In order to investigate the potentiality of such an ex-

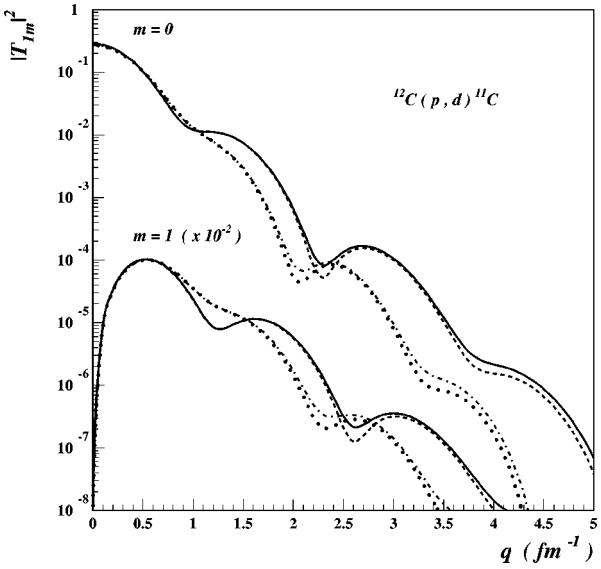

FIG. 2. Same as Fig. 1 for $|T_{1m}|^2$ with $m=0,1$.

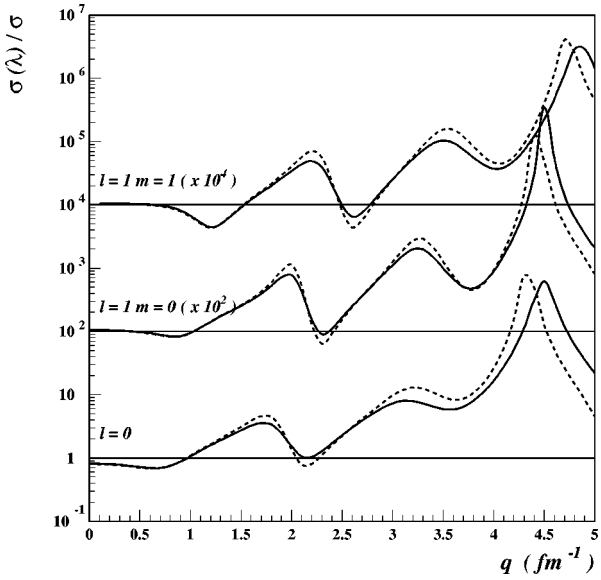

FIG. 3. Ratio $\sigma(\lambda)/\sigma$ of $|T_{lm}|^2$ calculated for $\lambda=k_d/k_p$ with respect to $\lambda=1$, for the three cases displayed in Figs. 1 and 2. The dotted line corresponds to the eikonal approximation; the solid line includes the first order correction.

pansion, we first simplify the optical potentials, setting

$$\frac{w_d}{k_d}V_d=\frac{w_p}{k_p}V_p=-\frac{i}{2}\sigma\rho_0 e^{-\beta^2 r^2}, \tag{25}$$

with $\rho_0=N\beta^3/\pi\sqrt{\pi}$, N being the number of nucleons in the target nucleus. Picking up the neutron in a $1s$ state, we have, up to irrelevant factors,

$$T_{00}(q)=\int bdbJ_0(qb)e^{-\gamma[t_0(b)+t_0(\lambda b)]} \times\int_{-\infty}^{\infty}dze^{iq_\parallel z}e^{\gamma[t_0(b)-t_0(\lambda b)]\mathrm{erf}(\beta z)}\Phi_{00}(b,z), \tag{26}$$

where

$$t_0(b)=e^{-\beta^2 b^2},\quad \gamma=\frac{\sigma}{4}\rho_0\frac{\sqrt{\pi}}{\beta}. \tag{27}$$

The Taylor expansion is readily obtained:

$$T_{00}(q)=T^{(0)}(q)+\sum_{n=1}^{\infty}\frac{(\lambda-1)^n}{n!}T^{(n)}(q), \tag{28}$$

where

$$T^{(0)}(q)=\int bdbJ_0(qb)e^{-2\gamma t_0(b)}\int_{-\infty}^{\infty}dze^{iq_\parallel z}\Phi_{00}(b,z) \tag{29}$$

and

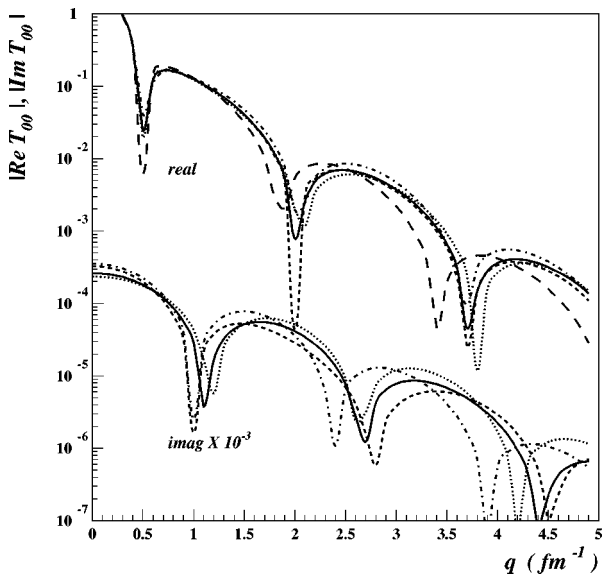

FIG. 4. Taylor expansion of $|T_{00}|$ around $\lambda=1$ (we recall that $\lambda=1.26$). Long dashed line: $T^{(0)}$ (note that the $\mathrm{Im}T^{(0)}=0$). Dot-dashed line: $T^{(0)}+T^{(1)}$. Dotted line: $T^{(0)}+T^{(1)}+T^{(2)}$. Dashed line: $T^{(0)}+T^{(1)}+T^{(2)}+T^{(3)}$. The solid line corresponds to the exact value.

$$T^{(n)}(q)=\sum_{j\leqslant n}\int b\,db J_0(qb)e^{-2\gamma t_0(b)}f^{nj}(b) \times\int_{-\infty}^{\infty}dz e^{iq_\parallel z}g^j(z)\Phi_{00}(b,z), \tag{30}$$

where $g^j(z)=[1+\mathrm{erf}(\beta z)]^j$ and

$$f^{11}(b)=2\gamma\beta^2b^2t_0(b),\quad f^{21}(b)=f^{11}(b)(1-2\beta^2b^2),$$
$$f^{22}(b)=f^{11}(b)^2,\quad f^{31}(b)=f^{11}(b)2\beta^2b^2(2\beta^2b^2-3),$$
$$f^{32}(b)=3f^{21}(b)f^{11}(b),\quad f^{33}(b)=f^{11}(b)^3.$$

This expansion is appealing but unfortunately $(\lambda-1)\ll 1$ is not sufficient as a convergence criterion. For instance, the strength constant γ plays also an important role. This can be checked from the first two contributions: starting from a spherically symmetric bound state wave function, $T^{(0)}$ has no imaginary part. The modulation by the mixed parity function $g(z)$ automatically induces an imaginary component in $T^{(1)}$ and, simultaneously, in the b variable, whereas in $T^{(0)}$ the optical potential produces a monotonic increase of the phase factor from nearly zero to unity, the function $f^{nj}(b)$ brings enhancement in the nuclear surface, an enhancement which get sharper with higher orders.

Once these two features are taken into account, the series converges reasonably well. Nevertheless, in practice, we find it necessary to go up to $T^{(3)}$ to come close to the exact value for $\lambda=1.26$, as illustrated by the curves of Fig. 4. For $\lambda=1.1$ the agreement is met only with $T^{(2)}$. Consequently we conclude that an expansion around $\lambda=1$ does not facilitate the task. Although, as stated above, this conclusion depends on γ and may be somehow better for a weak interaction, it underlines the fact that the λ effect cannot easily be estimated perturbatively.

IV. (p,d) REACTION ON HALO NUCLEI

We shall consider in this section the pickup of a neutron very weakly bound to a core. This situation can be identified with the ground state of single neutron halo nuclei. These last are characterized by a neutron separation energy, which is an order of magnitude smaller than the average binding energy per particle. As a consequence the description of such systems as two-body problems is justified, at least in a first approximation. Note that the same situation could occur in the spectrum of an ordinary nucleus near the threshold of neutron emission.

To fix ideas and perform practical calculations, we shall study the (p,d) transfer reaction on ^{11}Be, which is more or less the archetype of halo nuclei.

The formalism is basically the same as the one presented in the preceding section, up to a few modifications including c.m. corrections. On the one hand, we denote by $\vec{\xi}=(\vec{\beta},\sigma)$ the coordinate of the neutron with respect to the center of mass of the ^{10}Be core, whereas $\vec{r}=(\vec{b},z)$ is the coordinate of the incident proton. The impact parameter $\vec{b}$ is measured from the c.m. of ^{11}Be.

Furthermore, the halo neutron binding energy is so weak that it can undergo only a single interaction, leading either to dissociation or transfer. Consequently the phase factor of the entrance channel involves only a proton-core optical potential. Assuming as before a zero-range transfer profile function

$$\gamma^{dp}\left(\vec{b}-\frac{1}{1+\varepsilon}\vec{\beta}\right)=D_0\delta^{(2)}\left(\vec{b}-\frac{1}{1+\varepsilon}\vec{\beta}\right), \tag{31}$$

we end up with

$$T_{lm}(q)=D_0\int e^{i\vec{q}\cdot\vec{b}}d^2b \times\int_{-\infty}^{\infty}e^{iq_\parallel z}e^{i\chi_0(\vec{b},z)}\Phi_{lm}((1+\varepsilon)\vec{b},(1+\varepsilon)z)dz. \tag{32}$$

Here we have $\varepsilon=0.1$, the mass ratio between the halo neutron and the ^{10}Be core. On the grounds of the results of the preceding section we restrict the calculation of the distorting phase to the eikonal approximation. It is given by

$$\chi_0(\vec{b},z)=-\frac{\omega_p}{\hbar^2k_p}\int_{-\infty}^{z}V_p((\lambda+\varepsilon)\vec{b},z')dz' -\frac{\omega_d}{\hbar^2k_d}\int_{z}^{\infty}V_d(\vec{b},z')dz', \tag{33}$$

where V_p and V_d are the proton- and deuteron-^{10}Be optical potentials. According to Newton [12], we have introduced ω, the equivalent of the reduced mass:

$$\omega=\frac{w_1w_2}{w_1+w_2}. \tag{34}$$

TABLE II. Optical potential parameters for the ^{11}Be$(p,d)^{10}$Be reaction at 800 MeV [Eq. (37)].

	$V_p(r)$	$V_d(r)$
$V(0)$	56.95 MeV	24.24 MeV
κ	0.5964 fm^{-1}	0.4421 fm^{-1}
α	-0.2	-0.2

As in the preceding section, the optical potentials are constructed from the KMT prescription (20). The core is described by its one-body density

$$\rho_{\rm core}(r)=\frac{2\kappa^3}{5\pi\sqrt{\pi}}(1+\kappa^2r^2)e^{-\kappa^2r^2}, \tag{35}$$

normalized to 10 particles. We take $\kappa^2=0.3556$ fm^{-2}, corresponding to a charge rms radius of 2.43 fm for ^{10}Be, in agreement with the compilation of data by Angeli [16]. The two optical potentials read

$$V_j(r)=-V_j(0)(1+\kappa_j^2r^2)e^{-\kappa_j^2r^2}(i+\alpha_j)\quad(j=p,d). \tag{36}$$

The values of the parameters used in the calculations are listed in Table II.

Besides the influence of λ, which we want to check in this particular situation of the transfer of a loosely bound particle, our aim is to study the sensitivity of the differential cross section to the radial shape of the halo wave function. We assume the halo neutron to be in a $l=0$ state with respect to the core. In order to investigate a sufficiently large functional space, the following four cases have been selected.

(1) A difference of two Gaussians (no node) G_0

$$\Phi(\vec{\xi})=\left[\frac{\mu^2}{\pi}\right]^{3/4}\left[1+\frac{1}{3\sqrt{3}}-\frac{1}{\sqrt{2}}\right]^{-1/2}(e^{-\mu^2\xi^2/2}-e^{-3\mu^2\xi^2/2}), \tag{37}$$

with $\mu^2=0.0504$ fm^{-2}.

(2) A difference of two Gaussians with a node G_1,

$$\Phi(\vec{\xi})=\left[\frac{\mu^2}{\pi}\right]^{3/4}\left[1+\frac{B^2}{3\sqrt{3}}-\frac{B}{\sqrt{2}}\right]^{-1/2}(e^{-\mu^2\xi^2/2}-Be^{-3\mu^2\xi^2/2}), \tag{38}$$

with $\mu^2=0.0335$ fm^{-2} and $B=2.80$, this last being determined in order to get orthogonality with a single Gaussian of rms radius of the core size.

(3) and (4) are numerical solutions of the Schrödinger equation for a Woods-Saxon potential, the eigenvalue being equated with the neutron separation energy of ^{11}Be, namely, 0.5 MeV: WS_0 (no node) and WS_1 (one node). In the case of WS_1, the size of the potential is the one expected to describe ^{10}Be, so that this wave function is orthogonal to the $1s$ neutron state of the core. The antisymmetry problem is ignored in the case of WS_0, which is chosen essentially for its radial dependence.

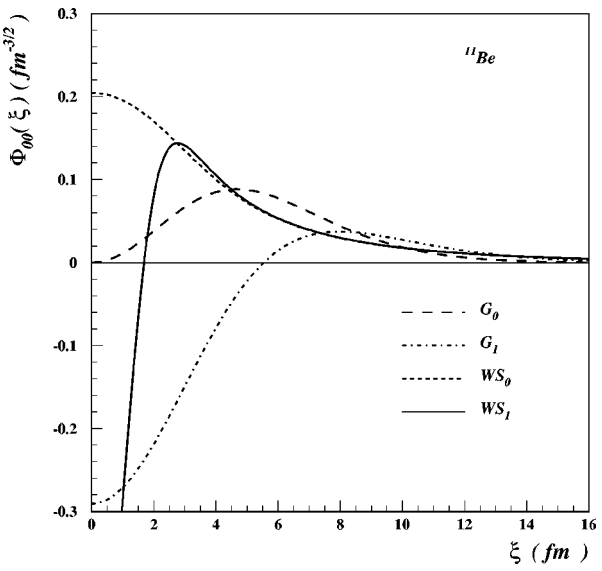

FIG. 5. The four neutron halo wave functions used in the present work. See text.

These four wave functions have the same rms radius, namely, 6.6 fm, in agreement with the experimental value [17]. They are displayed in Fig. 5.

The results of present calculations of $|T_{00}(q,q_\parallel)|^2$ are displayed in Figs. 6 and 7, for the Gaussian and the WS cases, respectively. The first obvious conclusion is the strong influence of λ (here $\lambda=1.255$) on the diffractive pattern. Thus, in spite of the fact that the halo wave function extends over large distances, with an important fraction outside the efficient range of the optical potentials, this effect cannot be neglected. On the other hand, the sensitivity of the differential cross section to the wave function is encouraging. Even below $q=2$ fm^{-1}, the difractive patterns are different enough to be selective. It means that owing to a reaction mechanism which is well under control, intermediate ener-

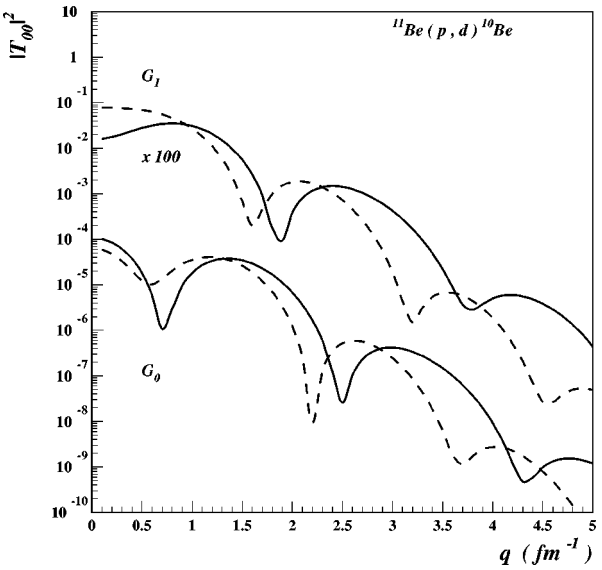

FIG. 6. (p,d) reaction on ^{11}Be at 800 MeV incident energy. $|T_{00}|^2$ in arbitrary units is plotted against q for the two halo wave functions G_0 and G_1 (see text). The dashed lines correspond to $\lambda=1$, the solid lines to $\lambda=k_d/k_p$.

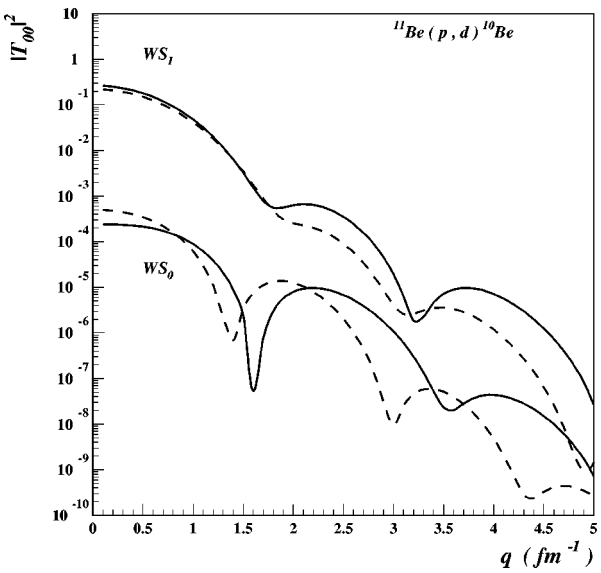

FIG. 7. Same as Fig. 6 for the two halo wave functions WS_0 and WS_1 (see text).

gies transfer reactions constitute indeed a powerful tool to study halo wave functions.

Another interesting feature is the dependence of $|T_{00}(q,q_\parallel)|^2$ on the rms radius of the halo wave function. To illustrate this point, we display in Fig. 8 calculations performed by using G_0 for three different values of the rms radius, namely, 4.6, 6.6, and 8.6 fm. On the one hand, we find $|T_{00}(q)|^2$ to decrease strongly with the radius. On the other hand, the diffractive nature of the scattering is well characterized by the shift of the minima towards lower q values as the radius increases.

The decrease of the transfer cross section with the rms radius of the halo wave function differs qualitatively from

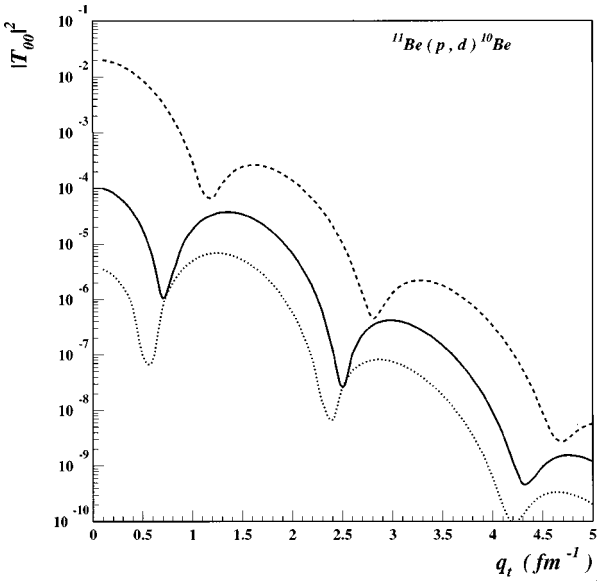

FIG. 8. (p,d) reaction on ^{11}Be at 800 MeV incident energy. Sensitivity of $|T_{00}|^2$ to the rms radius of the halo wave function. Use is made here of the wave function G_0 with the range parameter adjusted to $\langle r^2\rangle^{1/2} = 4.6$ fm (dashed line), 6.6 fm (solid line), and 8.6 fm (dotted line).

the behavior of the dissociation cross section. It would be very instructive to understand this situation on the grounds of a simplified model, similar to the one developed in Eqs. (28)–(30) taken at $q=0$. Setting $\lambda=1$, which is permissible for the present purpose, we are left with $T_{00}^{(0)}(0)$. In order to obtain analytical expressions we replace $e^{-2\gamma t_0(b)}$ by two simple forms

$$\text{(a)}\quad e^{-2\gamma t_0(b)} \rightarrow \mathrm{erf}(\alpha b),$$

with $\alpha=0.32$ corresponding to $\mathrm{erf}(\alpha b)=0.5$ at $b=1.5$, and

$$\text{(b)}\quad e^{-2\gamma t_0(b)} \rightarrow \theta(b_0-b),$$

with $b=2.0$ fm. Though not precise, these two forms are sufficient to simulate the strong absorption of the eikonal phase at low impact parameters and to give insight into the problem. By using the G_0 wave function, we get, up to irrelevant factors,

$$\text{(a)}\quad T_{00}^{(0)}(0,q_\parallel) \propto \langle r^2\rangle^{3/4}\left[\exp\left(-\frac{\langle r^2\rangle}{4.4(1+\varepsilon)^2}q_\parallel^2\right)\times\sqrt{\frac{2\langle r^2\rangle\alpha^2}{2.2(1+\varepsilon)^2+\alpha^2\langle r^2\rangle}}-\frac{1}{3\sqrt{3}}\exp\left(-\frac{\langle r^2\rangle}{13.2(1+\varepsilon)^2}q_\parallel^2\right)\times\sqrt{\frac{2\langle r^2\rangle\alpha^2}{6.6(1+\varepsilon)^2+\alpha^2\langle r^2\rangle}}\right],$$

$$\text{(b)}\quad T_{00}^{(0)}(0,q_\parallel) \propto \langle r^2\rangle^{3/4}\left[\exp\left(-\frac{\langle r^2\rangle}{4.4(1+\varepsilon)^2}q_\parallel^2\right)\times\exp\left(-\frac{4.4(1+\varepsilon)^2}{\langle r^2\rangle}\right)-\frac{1}{3\sqrt{3}}\exp\left(-\frac{\langle r^2\rangle}{13.2(1+\varepsilon)^2}q_\parallel^2\right)\times\exp\left(-\frac{13.2(1+\varepsilon)^2}{\langle r^2\rangle}\right)\right].$$

Use is made here of $\mu^2=2.2\langle r^2\rangle^{-1}$. From a few numerical estimates, it is easy to become convinced that in both cases, the decrease of $T_{00}^{(0)}$ is merely dictated by the second factor. It suggests that, in the case of halo nuclei, transfer reactions on heavier nuclei like (^{3}He,^{4}He), involving smaller $q_\parallel$, could be more efficient having larger cross sections.

V. CONCLUSIONS

The present work deals with (p,d) transfer reactions formulated in the Glauber approach. If the incident energy is high enough that the eikonal approximation is valid, the reaction mechanism appears to be well under control, provided that the change in the impact parameter at the transition vertex is taken into account. This effect is not negligible and

cannot be easily treated perturbatively. On the specific example of (p,d) on ^{12}C at 800 MeV incident energy, at large momentum transfer, this effect brings corrections to $|T_{lm}(q,q_\parallel)|^2$, reaching up to two orders of magnitude. By comparison, at this energy, contributions arising from noneikonal propagation play a minor role. Interference with the Coulomb phase, on the other hand, has no decisive importance.

As far as halo nuclei are concerned, together with a large longitudinal momentum transfer, the very small separation energy constitutes a strong argument in favor of single step transfer reactions, which may not hold in general. We find the differential cross section to be rather sensitive to the radial shape of the halo wave function. Thus, the intermediate energy (p,d) reaction could be a useful tool to measure the halo wave function, to the extent that the optical potentials in both the entrance and exit channels are well determined. As advocated by Wilkin in his quoted paper [1], this process has the priviledge of testing the wave function at large momenta, which is always a challenging problem. Furthermore, since the magnitude of the cross section is found to be decreasing strongly with the longitudinal component of the momentum transfer and the radius of the halo wave function, (^{3}He,^{4}He) processes may be more advantageous than the (p,d) reaction, except that multiple step processes may spoil the analysis in the case of low $q_\parallel$.

Finally, we emphasize that the use of optical potentials in the entrance and exit channels is more efficient than microscopic calculations based on the nucleon-nucleon profile functions. This is due to the fact that above the pion production threshold, Δ production is rapidly increasing, giving rise to a series of complicated processes in the intermediate steps of the particle propagation. The optical potential, when taken from experiment, will automatically sum the corresponding diagrams.

ACKNOWLEDGMENTS

One of us (F.C.) expresses his thanks to the French MESR for its financial support and the division de physique Théorique de l'IPN d'Orsay for its kind hospitality. Division de Physique Théorique is a ''Unité de Recherche des Universités Paris 11 et Paris 6 Associée au CNRS.''

[1] C. Wilkin, J. Phys. G **6**, 69 (1980).
[2] J. R. Shepard and E. Rost, Phys. Rev. C **25**, 2660 (1982).
[3] R. D. Amado, J. P. Dedonder, and F. Lenz, Phys. Rev. C **21**, 647 (1980).
[4] B. F. Bayman, S. M. Lenzi, A. Vitturi, and F. Zardi, Phys. Rev. C **50**, 2096 (1994).
[5] J. Formanek, Czech. J. Phys. **26**, 842 (1976); **30**, 726 (1980).
[6] C. Lazard, R. J. Lombard, and Z. Maric, J. Phys. G **11**, 991 (1985).
[7] C. Lazard, R. J. Lombard, and Z. Maric, J. Phys. G **13**, 321 (1987).
[8] C. Lazard and R. J. Lombard, *Eikonalized model for transfer reaction*, in *Jubilej Zvonka Marica* (in serbian), Lectures in physical sciences (SFIN), Volume V, No. 2 (Institute of Physics, Belgrade, 1992), p. 1.
[9] J. Formanek and R. J. Lombard, J. Phys. G **23**, 423 (1997).
[10] S. J. Wallace, Ann. Phys. (N.Y.) **78**, 190 (1973).
[11] D. Waxmann, C. Wilkin, J.-F. Germond, and R. J. Lombard, Phys. Rev. C **24**, 578 (1981).
[12] R. Newton, *Scattering of Waves and Particles*, 2nd ed. (McGraw-Hill, New York, 1982).
[13] A. K. Kerman, H. Mc Manus, and R. M. Thaler, Ann. Phys. (N.Y.) **8**, 551 (1959).
[14] A. Chaumeaux, V. Layly, and R. Schaeffer, Ann. Phys. (N.Y.) **116**, 247 (1978).
[15] L. Ray, Phys. Rev. C **19**, 1855 (1979).
[16] I. Angeli, J. Phys. G **17**, 439 (1991).
[17] See, for instance, D. V. Fedorov, A. S. Jensen, and K. Riisager, Phys. Lett. B **312**, 1 (1993).